https://doi.org/10.46813/2023-148-090

GENERATION OF COMPENSATED ION-ELECTRON FLOW IN THE COMBINED MAGNETRON-ION-PLASMA SYSTEM

A. Zykov, N. Yefymenko, S. Dudin, S. Yakovin, N. Azarenkov
V.N. Karazin Kharkiv National University, Kharkiv, Ukraine
E-mail: zykov@karazin.ua

The design and characteristics of the combined Magnetron-Ion-Plasma System (MIPS) are presented. The system includes a magnetron sputtering system and a Hall-type ion source with a common magnetic system and common power supply allowing the generation of quasi-neutral ion-electron flow, which provides complete charge neutralization on the processed dielectric surface. The formation of the anode electron layer and the energy spectra of ions are experimentally investigated. A phenomenological model of the combined discharge in EH fields is proposed. Theoretical calculations and experimental data are in reasonable agreement.

PACS: 52.77.-j, 81.15.-z

INTRODUCTION

Formation of nanostructured coatings on heat-sensitive materials, internal stresses control and damage reduction in the synthesized films, and other modern technological challenges give rise to the demand for ion flow generation towards the surface of the growing film of relatively low energy (1…200 eV) with the ability of fine-tuning, and with controllable current density in the range 0…10 mA/cm^2. When dielectric coatings are deposited, an additional condition of charge neutralization on the film surface arises [1, 2].

The combined low-energy Magnetron-Ion-Source Sputtering System (MISSS), which is presented in [3, 4], is primarily intended for the synthesis of hard coatings with high plasticity in the conditions of high non-equilibrium energy flux per condensed atom of 10…1000 eV/at. (referring to the Thornton diagram [5]). However, for the synthesis of coatings in the region of small values of this parameter (less than 10 eV/at.), it had been necessary to rearrange the design of the ion source. The main goal of the system reconstruction was to allow the low-voltage operation mode of the Hall-type ion source and to develop effective means of current density control of the generated ion-electron flow.

The previous paper [6] presented the design of the new modification of the system, which is the combined Magnetron-Ion-Plasma System (MIPS), and the results of experimental studies of magnetron discharge (MD) ignition and the plasma mode of operation of the Hall-type ion source (IS) in dependence on the gas pressure and the strength and topology of the magnetic field. The current-voltage characteristics of MD and IS during their autonomous and joint operation were also measured, and their mutual influence was studied. The described research was performed with two separate power supplies for MD and IS, which is convenient for research but single-supply operation would be preferable for real-life technology applications.

The present research is focused on the study of the characteristics of MIPS for powering the MD and IS from a common power supply, particularly, in the case when it is electrically isolated from the chamber. The distribution of low-energy ion flow between the sample table and other electrodes is also studied together with energy spectra of ions, and the influence of external factors on these values. The problem is treated both experimentally and theoretically.

1. EXPERIMENTAL SETUP

The scheme of the magnetron-ion-plasma system (MIPS) modified for operation in the plasma mode is presented in Fig. 1. In comparison with the magnetron-ion-source sputtering system [3], in this design, the output channel of the ion source was expanded to 15 mm and the anode was shifted toward the output of the source. The optimization of the anode location and geometry as well as the geometry of the output channel of the source (being part of the magnetic core) was carried out in accordance with the topology of the magnetic field lines (MFL) calculated using the COMSOL Multiphysics 5.6 software (Fig. 2).

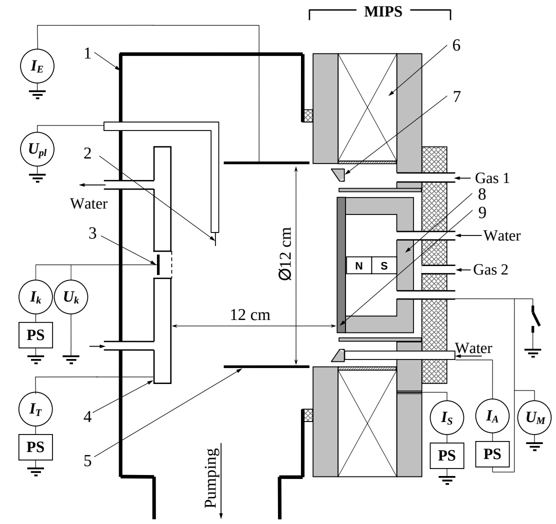

Fig. 1. Scheme of MIPS:
1 – vacuum chamber; 2 – probe; 3 – RFEA;
4 – sample table; 5 – bounding electrode; 6 – solenoid;
7 – anode; 8 – magnetron; 9 – target

An additional isolated cylindrical electrode with a diameter of 120 mm and a length of 60 mm was mounted in the chamber in order to localize the plasma between the magnetron and the sample holder table and to study ion current distribution between the electrodes of the MIPS.

A Langmuir probe was located in the plasma to measure the plasma potential. In fact, just the floating potential of the probe was measured, which was approximately assumed as the plasma potential. A single-grid retarding-field energy analyzer (RFEA) was mounted behind the central hole (diameter 5 mm) in sample table for measuring ion energy spectra.

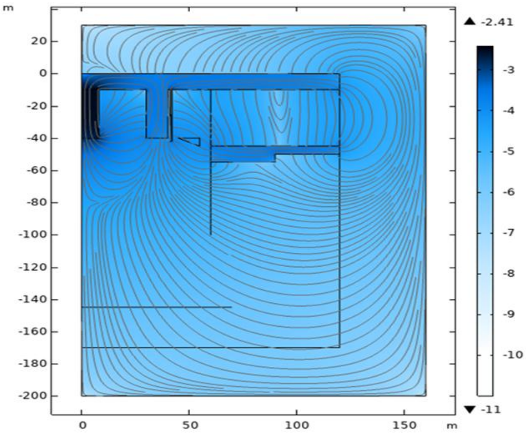

Fig. 2. The topology of the magnetic field lines in MIPS (I_S = 2 A)

2. EXPERIMENTAL RESULTS

2.1. CURRENT-VOLTAGE CHARACTERISTICS

The main focus of current research is the operation of both parts of MIPS (magnetron and ion source) from a single power supply. The supply is connected between the anode and the magnetron (see Fig. 1) but two different modes of operation are possible: i) with grounded magnetron (GM); ii) with floating magnetron (FM). The latest mode allows the generation of quasi-neutral ion-electron flow, which is especially important for non-conductive coating deposition.

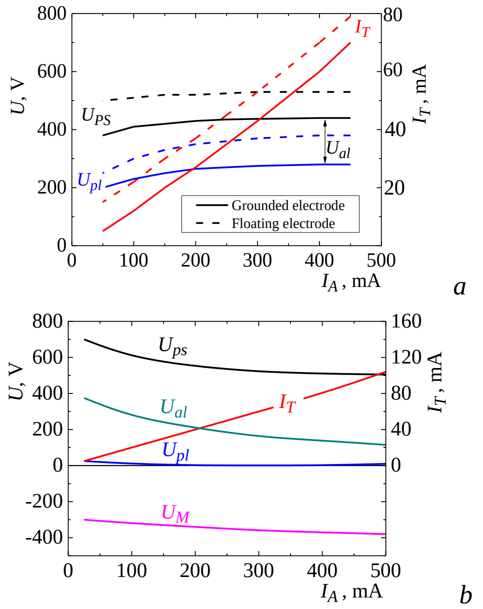

Fig. 3. Current-voltage characteristics of MIPS in the operation modes with grounded (a) and floating (b) magnetron. I_S = 1.25 A, p = 1.2 mTorr

Fig. 3 shows the current-voltage characteristics (CVC) of MIPS in both modes. In GM mode (see Fig. 3,a), the anode voltage U_A, which is equal to the power supply voltage U_{PS}, slightly varies around 400 V and is almost independent on the discharge current. The plasma potential is $U_{pl} \approx (0.5\ldots0.75)\ U_a$. Ion current to the sample table is the important parameter characterizing the ion bombardment of the growing coating.

Fig. 3 demonstrates that the table current I_T (the saturation value of the ion current to the table with the bias of -30 V) amounts to 15…20% of the discharge current I_A and is proportional to it.

An additional bounding electrode (see Fig. 1) is introduced to the system in order to localize the plasma in the finite volume between the magnetron target and the sample table. The electrode may be grounded or floating. The latest case is useful for modeling the situation when the vacuum chamber walls became non-conductive during dielectric coating deposition. Fig. 3,a shows that the presence of an isolated additional electrode leads to a significant increase in the anode voltage and the plasma potential.

Ion acceleration within the ion source is defined by the voltage drop on the anode layer U_{al}, which is equal to the difference U_a - U_{pl}. U_{al} dependence on the discharge current is shown in Fig. 3. One can see that U_{al} is almost constant (about 200 V) in GM mode while it falls from 400 V to about 50 in FM mode.

2.2. IMPACT OF MAGNETIC FIELD STRENGTH

Dependences shown in Fig. 3 are taken at a fixed value of the magnetic coil current 1.25 A. However, the magnetic field strength in the vicinity of the anode (note that the magnetic field near the magnetron target is sourced mostly from the permanent magnet) affects MIPS parameters significantly. Fig. 4 reveals this influence, which is different in GM and FM modes. In the GM mode (see Fig. 4,a) the anode voltage and the plasma potential are almost independent of the magnetic coil current while the current distribution between the electrodes of the system depends on the magnetic field.

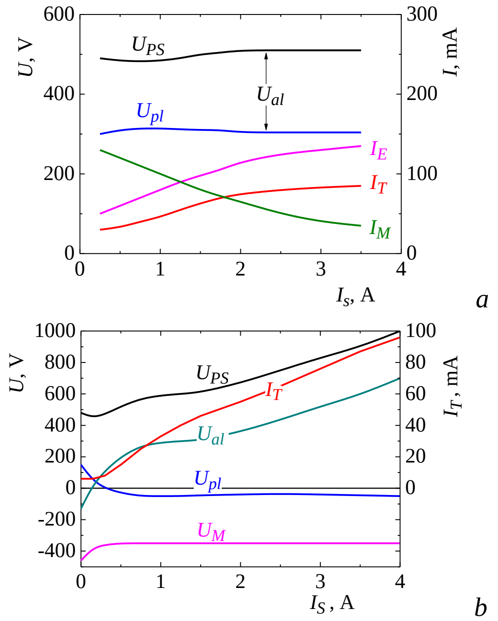

Fig. 4. Dependences of MIPS parameters on magnetic coil current in GM (a) and FM (b) modes. I_A = 300 mA, p = 0.9 mTorr (a); I_A = 200 mA, p = 1.5 mTorr (b)

It should be noted that in GM mode, the table, the magnetron target, the bounding electrode, and the chamber walls act as a united cathode collecting ion current both from the plasma and from the anode layer.

One can see from Fig. 4,a that in a weak magnetic field, the current flows predominantly to the magnetron target while with the growth of the magnetic field, the currents are redistributed in favor of the sample table and the bounding electrode.

The fundamental change in the dependence of the discharge voltage on the solenoid current due to the disconnection of the magnetron from the ground is seen from the comparison of Fig. 4. The magnetic field does not affect the magnetron voltage U_M significantly while the anode layer voltage U_{al} increases from -100 V to about 700 V, and in the range I_S = 0.75…4 A it grows almost proportionally to magnetic coil current. This means that at a weak magnetic field, the anode contacting with the plasma behaves as a usual anode of magnetron discharge with low voltage drop in the anode layer. However, the stronger magnetic field causes stronger magnetic insulation of the anode from the plasma attributed to the growth of the voltage drop in the anode layer U_{al}.

Let us summarize the main features of the formation of self-consistent potentials of the electrodes of MIPS. In GM mode (see Figs. 3,a and 4,a), the power supply voltage is almost independent on the discharge current and the magnetic field and is usually of 400…500 V (note that the power supply operated as a current source). The distribution of this voltage between anode and cathode layers (in roughly equal portions) is also almost independent on the discharge current and magnetic field strength. However, in FM mode the power supply voltage is not constant anymore, and its distribution between anode and cathode layers is highly dependent on parameters, especially on the magnetic field strength near the anode.

2.3. ION ENERGY DISTRIBUTION

Ion current to the sample table (see Figs. 3, 4) is the important parameter characterizing the ion bombardment of the growing coating but the ion energy is of no lesser importance. Thus, the ion energy distribution function was estimated by means of a retarding-field energy analyzer (RFEA) installed at the center of the sample table. The front grid of the RFEA was connected to the table, and both were biased at -100 V in order to suppress electron current from the plasma.

The braking characteristics of the ion current from the plasma (Fig. 5), confirm that the main part of the ions are generated in the plasma and, accordingly, have an energy close to U_{pl}. At the same time, the ion energy spectrums possess high-energy "tails" reaching the anode potential U_A. In the GM mode, the plasma potential is relatively high causing high ion energy (300…400 eV), which is even greater in the case of the floating boundary electrode (see dashed line in Fig. 5,a). The braking characteristics of the ions hitting the sample table are presented in Fig. 5,b for different solenoid currents I_S. One can see that by adjusting the magnetic field it is possible to effectively control the high-energy component of the ion spectrum, both in terms of energy and current density. Note that in FM mode, the high-energy ions coming from the anode layer demonstrate approximately linear dependence of the distribution function on energy.

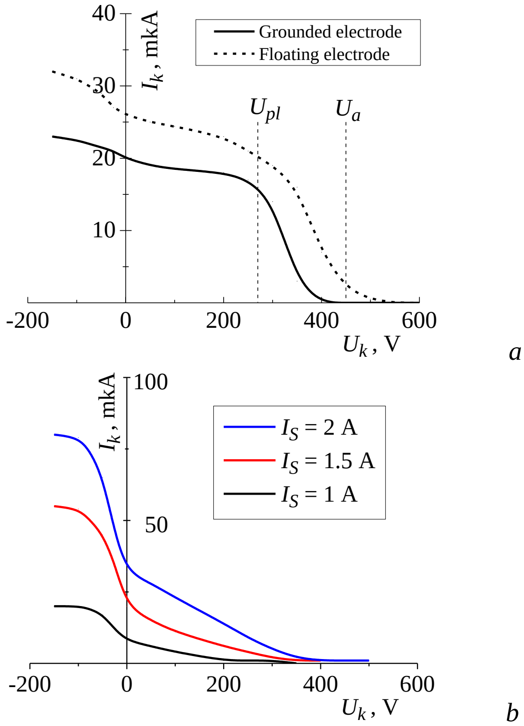

Fig. 5. Braking characteristics of the ion flow to the sample table in GM (a) and FM (b) modes. I_A = 300 mA; p = 0.9 mTorr

3. THEORETICAL MODEL OF MIPS

In the previous section, it was shown that MIPS exhibits rather complex behaviour. It is a system with several electrodes, voltages and currents on which are set automatically and self-consistently depending on the magnetic field. In this section, we will build a simple model that describes the main regularities in the formation of system parameters.

In the model, the system includes 4 electrodes and plasma, which is in direct contact with all the electrodes (Fig. 6). Two of these electrodes, the cathode (magnetron target) and the anode of the ion source, are isolated from the plasma by a transverse magnetic field.

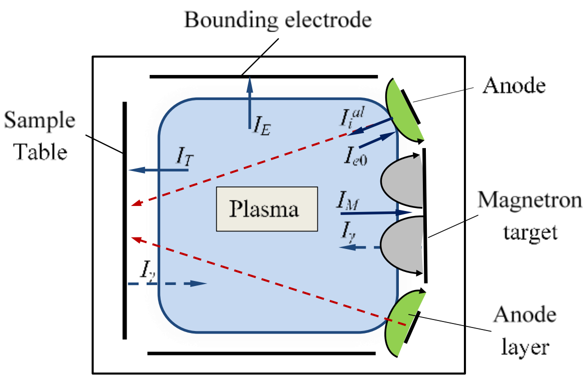

Fig. 6. Schematic diagram of the arrangement of electrodes and the distribution of charged particle currents according to the spatially averaged MIPS model

All electrodes are negative relative to the plasma, except for the anode, near which, due to magnetic isolation, an anode layer is formed, and the anode potential is positive relative to the plasma. Due to the presence of the anode layer, an ion flow can be formed, which is directed toward the sample table. A cathode layer is formed between the plasma and the magnetron target, in which the ions are accelerated, sputtering the target. For simplicity, the plasma in the model is assumed to be equipotential and homogeneous, in other words, we are building a spatially averaged model like a Global model in [7].

We emphasize that there are two regions of ionization in the system (plasma and anode layer) interacting with each other. The electron current from the plasma is the seed current for the anode layer. As a result of ionization amplification, the electron current increases up to the anode current, and the ions produced in the layer are pushed out into the plasma. In turn, the ion current from the anode layer to the plasma contributes to the magnetron discharge, which leads to a decrease in the equilibrium cathode voltage.

The system is governed by two parameters, namely the power supply voltage (applied between the cathode and anode) and the magnetic field strength in the ion source gap, which is determined by the solenoid current. Depending on the magnetic field, the applied voltage is self-consistently redistributed between the anode and cathode layers, and the flux of charged particles born in the plasma and in the anode layer is redistributed between the electrodes of the system. The purpose of the model is to justify the patterns of this redistribution derived from the experimental results.

The model is based on the balance equations of particles and energy, and the drift model of the anode layer in crossed EH fields following the logic of [7, 8]. The spatially averaged model of magnetron discharge [7] may be presented in the form:

$$U = \frac{\eta_{pl}}{e\gamma}, \tag{1}$$

where U is the discharge voltage, η_{pl} is the energy cost of an ion creation, γ is ion-electron emission coefficient. The concept of ionization cost is frequently used to describe cumulative energy losses per ion-electron pair created [9, 10]. Generally, it depends on electron energy distribution function and its value is different for different specific kinds of plasmas. Since the ionization in MIPS appears in two regions with different conditions, we use two different values of the ionization cost for the plasma and the anode layer, η_{pl} and η_{al}, respectively.

Taking into account the mentioned above mutual influence of the plasma and the anode layer, the plasma potential U_{pl} (which is the magnetron discharge voltage) is defined by equation (1) but with an additional factor taking into account the bombardment of the electrodes by ions generated in the plasma I_i^{pl} and in the anode layer I_i^{al}:

$$eU_{pl} = \frac{\eta_{pl}}{\gamma} \frac{I_i^{pl}}{I_i^{pl} + I_i^{al}}. \tag{2}$$

A one-dimensional drift model of the electron current in crossed *EH* fields is used to describe the anode layer with ionization amplification of the seed electron current from the plasma, which is analogous to the Townsend theory. Adopting the approach of [10], and assuming that the electric field E is directed along the x-axis to the surface of the anode, and the magnetic field H is parallel to the anode surface, the 1D conservation equation of the electron current density j_e can be written in the form:

$$\frac{dj}{dx} = \frac{E}{\eta_{al}} \cdot j_e, \tag{3}$$

where η_{al} is the ionization cost in a strong electric field in anode layer.

It should be noted that we are dealing here with low-voltage anode layer where the voltage is not sufficient for electron avalanche developing, and only the seed electrons can produce ionization in the layer. Assigning the seed current density as j_{e0} and using the equation $E = d\varphi/dx$, the relationship between the current density j and potential φ in the anode layer can be obtained from the equation (3). Under the boundary conditions $x = 0$; $j_e = j_0$; $\varphi = \eta_{al}$ it has the form:

$$j_e = \frac{\varphi}{\eta_{al}} \cdot j_{e0}. \tag{4}$$

In the model (as in the experiment), the power supply is always connected between the magnetron and the anode but we consider two modes of MIPS operation: with grounded magnetron (GM) and with floating magnetron (FM). Fig. 7 illustrates the difference in potential distributions in these two modes. The right side of the curves has two branches representing the two ways of measuring: plasma – anode and plasma – magnetron target.

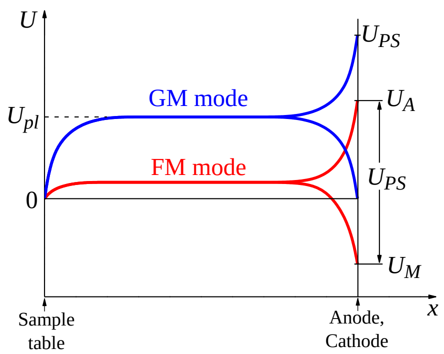

Fig. 7. Qualitative potential distribution in GM mode (blue line) and FM mode (red line)

In the GM mode, all the electrodes bounding the plasma (excluding the anode) are under ground potential. Taking into account the anode surface area is much less than the total cathode surface, this mode may also be named as "hollow-cathode mode".

In this mode, plasma electrons are insulated from the cathodes by the potential barrier of hundreds Volts, so the only way to escape for them is towards the anode, which is positive vs plasma. These electrons enter the anode layer forming the seed current I_{e0}. The value of I_{e0} is equal to the number of ions hitting the grounded electrodes. The current of ions born in the anode layer and flying into the chamber I_i^{al} and the opposite flow of electrons from the plasma

$$j_{e0} = I_\gamma + I_i^{pl} = \gamma I_i^{pl}\left(1+\frac{I_i^{al}}{I_i^{pl}}\right) + I_i^{pl} \qquad (5)$$

ensure the relationship of these regions. Considering $I_i^{al} = I_{e0}(U_{al}/\eta_{al} - 1)$ it is possible to write:

$$\frac{U_{pl}}{\eta_{pl}} = \frac{\eta_{al}}{\eta_{pl}}\frac{1+1/\gamma}{U_{al}/\eta_{al}} - 1. \qquad (6)$$

As a result, for the normalized discharge voltage U_{PS}/η_{pl}, we have the dependence on the voltage drop in the anode layer U_{al}:

$$\frac{U_{PS}}{\eta_{pl}} = \frac{U_{al}}{\eta_{pl}} + \frac{U_{pl}}{\eta_{pl}} = \frac{U_{al}}{\eta_{pl}} + B\left(\frac{1+1/\gamma}{U_{al}/\eta_{al}} - 1\right), \qquad (7)$$

where $B = \eta_{al}/\eta_{pl}$ is a constant coefficient, determined by the ratio of the ionization costs in the anode layer and in the plasma.

Fig. 8 presents graphically the dependences of the normalized power supply voltage on the normalized potential drop in the anode layer according to equation (7) for different γ in the case $B = 1$. With the anode layer absent ($U_{al}/\eta_{pl} \rightarrow 1$), for example, when there is no magnetic insulation of the anode, the voltage increases to the value $U_{pl} = (\eta_{pl}/\gamma)$, which corresponds to the existence of only magnetron discharge.

In the figure, the dotted lines indicate the potential drop in the cathode layer (U_{pl}/η_{pl}), which corresponds to the plasma potential relative to the cathode. Note that in this mode the value (U/η) depends significantly on the flow of ions and electrons to the bounding electrode consistently with the experimental results.

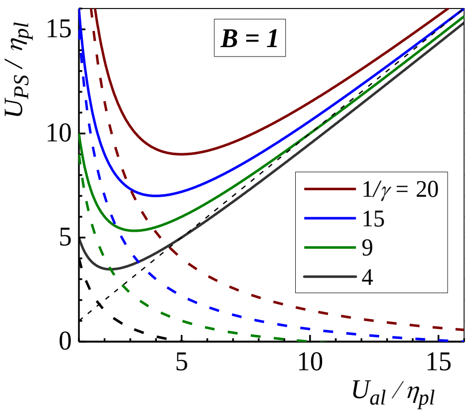

Fig. 8. Dependences of the normalized power supply voltage on the normalized potential drop in the anode layer according to equation (7) for different γ in the case B = 1. Dotted lines determine the potential drop in the cathode layer U_{pl}/η_{pl}

The most interesting and important point shown by Fig. 8 is the presence of a minimum discharge voltage in the entire range of parameters with the simultaneous existence of cathode and anode layers of space charge. Generally, the U_{pl}/U_{al} ratio is a free parameter but, from the comparison with the experimental data, we have made the conclusion that the system always self-consistently chooses the regime with the minimum possible U_{PS} similarly to glow discharge trending to the Stoletov's point with the most efficient ionization [10].

In FM mode the power supply is connected between the anode and the magnetron but is completely insulated from any other electrode and ground. Since no net current can flow out of the union of the magnetron with the ion source, a completely current-compensated ion-electron flow is generated towards the sample table. This mode of operation of the system can be named as a "plasma source mode". In this case, as it was mentioned in the experimental section, the fundamental change in the dependence of the discharge voltage on the solenoid current appears, and the question arises, what mechanism determines how many electrons from the plasma are injected into the attractive layer and, accordingly, how many ions are generated?

If we normalize the equations by the values

$$\rho^2 = \frac{2\eta_{al}}{m_e e\omega_H^2},\ E_0 = \frac{\eta_{al}}{e\rho},\ I_H = \frac{9\nu E_0}{4\pi},$$

then it is possible to obtain from equation (4) a solution for U_{al}/η and I_e/I_{e0} as a function of x:

$$\frac{U_{al}}{\eta_{al}} = \frac{I_{e0}}{I_H}\left(\frac{x}{\rho}\right)^3;\ \frac{I_e}{I_{e0}} = \frac{I_{e0}}{I_H}\left(\frac{x}{\rho}\right)^3, \qquad (8)$$

where $I_H = 9\nu\eta_{al}/(4\pi e\rho)$ is the value that normalizes the discharge current. Using the boundary condition at $x = \rho_0$ as $U_{al} = \eta_{al}$; $I_e = I_{e0} = I_H$, based on the magnitude of the discharge current, it is possible to determine the minimum value of the magnetic field H_0 for the formation of the anode layer and the maximum thickness of the layer ρ_0.

If in the "plasma source" mode, the thickness of the anode layer is considered to be a constant value ($\rho = \rho_0 = const$), then at a fixed discharge current ($I_e = const$) the dependence of the voltage drop in the anode layer U_{al} and the current of primary electrons from the plasma I_{e0} on the magnetic field is revealed, namely:

$$\frac{U_{al}}{\eta_{al}} = \left(\frac{H}{H_0}\right); \qquad \frac{I_{e0}}{I_e} = \left(\frac{H_0}{H}\right).$$

Thus, having represented the Larmor radius of electrons in the form $\rho = \rho_0(H_0/H)$, equation (8) takes the form:

$$\frac{U_{al}}{\eta_{al}} = \frac{I_e}{I_{e0}} = \left(\frac{x}{\rho_0}\right)^3\left(\frac{H}{H_0}\right). \qquad (9)$$

Graphs of the function (9) with different values of the parameters H/H_0 and x/ρ_0 in the range $x/\rho_0 < 1$ are presented in Fig. 9.

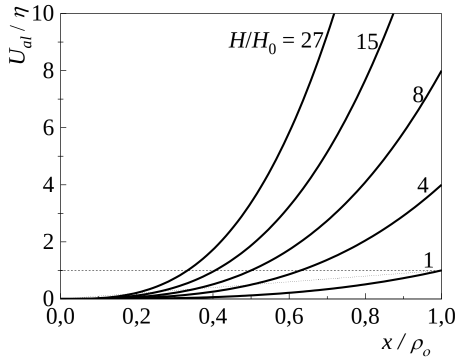

Fig. 9. Distribution of the normalized potential drop in the anode layer in the "plasma source" mode at different magnitudes of the magnetic field (H/H_0). $\rho = const$

CONCLUSIONS

In the present research, the characteristics of the combined Magnetron-Ion-Plasma System (MIPS) were studied both experimentally and theoretically. The system includes a magnetron sputtering system and a Hall-type ion source with a common magnetic system and common power supply allowing the generation of quasi-neutral ion-electron flow. The comparative analysis of the results of experimental studies and calculations according to the phenomenological model of MIPS has shown the following.

The proposed system model took into account the simultaneous existence of two regions with intense ionization of the working gas, the magnetron plasma and the anode layer. According to the model, the interaction of these regions appears due to the current of primary electrons from the plasma into the anode layer and to the current of ions from the anode layer.

The applied voltage distribution between anode and cathode layers is formed self-consistently keeping the system in the energetically optimal operating mode with the maximum current and the minimum discharge voltage. The presence of this optimal voltage explains the stabilized character of the discharge CVC, and the estimation of the value of the plasma potential corresponds well to the experimental data.

The value of the anode potential drop determines the value of the current of seed electrons from the plasma to the anode layer and the current of ions into the plasma regardless of the magnetic field.

Studies of energy spectra of ions confirm the calculated potential distribution in the system.

The influence of the magnetic field strength is most evident when the power supply is isolated from the camera. In this case, the strength determines the voltage drop in the anode layer and the ion current. A completely current-compensated ion-electron flow is generated towards the sample table.

It is important that with such a setup of the system, the negative potential of the magnetron versus the chamber is automatically set to the level, which ensures the injection of an electron flow from the plasma into the anode layer with the value that is equal to the ion flow from the plasma to the anode layer.

In general, the model qualitatively and quantitatively explains the main characteristics of the combined MIPS operation from external parameters: working gas pressure, electric power and magnetic field.

The obtained results can be applied to discharges with different geometries of electrodes with crossed EH fields, namely, Penning discharge, cylindrical ion magnetron, Hall-type ion source “Radical”, end Hall accelerator and others.

ACKNOWLEDGEMENTS

This research was supported by the National Research Foundation of Ukraine in the framework of the project 2021.01/0204.

REFERENCES

1. J. Reece Roth. *Industrial Plasma Engineering: Application to Nonthermal Plasma Processing*. CRC Press. 2001, v. 2, № 2, p. 645-651.
2. J. Musil. Hard nanocomposite coatings: Thermal stability, oxidation resistance and toughness // *Surf. Coat. Technol.* 2012, v. 207, № 1, p. 50-65.
3. A. Zykov et al. *Combined Magnetron-Ion-Source System for Reactive Synthesis of Complex Nanostructured Coatings, In: A. Pogrebnjak, O. Bondar (eds) Microstructure and Properties of Micro- and Nanoscale Materials, Films, and Coatings (NAP 2019)*. Springer Proceedings in Physics, Springer, Singapore, 2020, v. 240, p. 161-175.
4. A. Zykov, N. Yefymenko, S. Dudin, S. Yakovin. Discharge characteristics of combined low energy ion source – magnetron sputtering system // *Problems of Atomic Science and Technology. Series “Plasma Physics”*. 2020, № 6, p. 169-173.
5. A. Anders. Structure zone diagram including plasma-based deposition and ion etching // *Thin Solid Films.* 2010, v. 15, p. 4087.
6. A. Zykov, N. Yefymenko, V. Korneenkov, S. Dudin, and S. Yakovin. The Energy and Ion Flux Control in MISSS for Nanostructure Coating Synthesis // *IEEE 11th International Conference Nanomaterials: Applications and Properties (NAP)*, Odessa, Ukraine, 2021, p. 1-5.
7. M.A. Lieberman and A.J. Lichtenberg. *Principles of Plasma Discharges and Materials Processing, 2nd ed.* New York, Wiley, 2004, p 575.
8. A.V. Zykov, S.V. Dudin, S.D. Yakovin. Teady-state regimes of low-pressure magnetron discharge // *Physical surface engineering.* 2015, v. 13, № 2, p. 264-275.
9. S.V. Dudin, A.V. Zykov, K.I. Polozhi, V.I. Farenik. Ion energy cost in a combined inductive-capacitive rf discharge // *Tech. Phys. Lett.* 1998, v. 24, № 11, p. 881.
10. S.O. Macheret, M.N. Shneider, R.C. Murray, and R.B. Miles. Ionization in Strong Electric Fields and Dynamics of Nanosecond-Pulse Plasmas // *43rd AIAA Aerospace Sciences Meeting and Exhibit*, Reno, Nevada, January 10-13, 2005, p. 1.

Article received 19.06.2023

ГЕНЕРАЦІЯ КОМПЕНСОВАНОГО ІОН-ЕЛЕКТРОННОГО ПОТОКУ В КОМБІНОВАНІЙ МАГНЕТРОННІЙ ІОННО-ПЛАЗМОВІЙ СИСТЕМІ

О. Зиков, Н. Єфименко, С. Дудін, С. Яковін, М. Азарєнков

Представлено нову комбіновану магнетронну іонно-плазмову систему для синтезу наноструктурних покриттів на термочутливі матеріали. Експериментально досліджено формування прианодного електронного шару і енергетичних спектрів іонів у плазмовому режимі роботи системи. Запропоновано феноменологічну модель і механізм комбінованого розряду в ЕН-полях. Проведено порівняння теоретичних розрахунків і експериментальних даних.